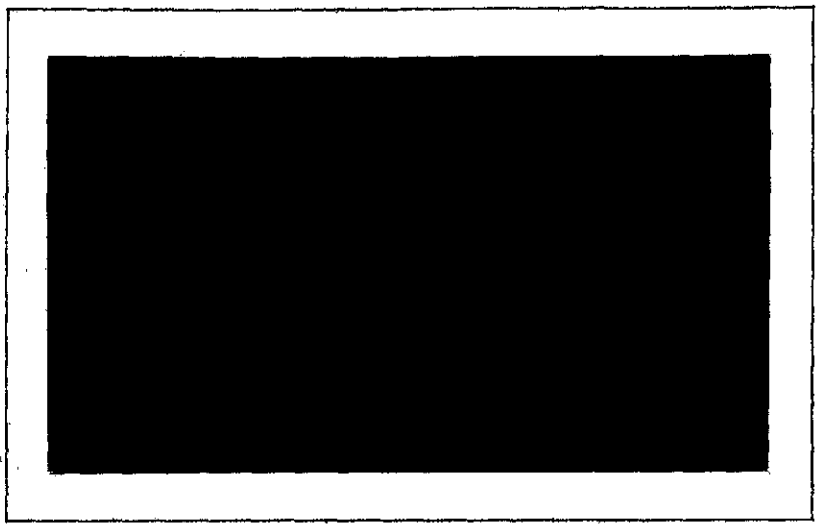

METALS RESEARCH LABORATORY

CARNEGIE INSTITUTE OF TECHNOLOGY

Carnegie-Mellon University

PITTSBURGH, PENNSYLVANIA

National Aeronautics and Space Administration
Research Grant NGR 39-087-003

THE EFFECT OF MICROSTRUCTURE AND STRENGTH ON THE FRACTURE TOUGHNESS OF AN 18 Ni, 300 GRADE MARAGING STEEL

by

J. A. Psioda and J. R. Low, Jr.

Department of Metallurgy and Materials Science
Carnegie-Mellon University
Pittsburgh, Pennsylvania 15213

NASA Technical Report No. 6

August 1974

This investigation was made possible by a Research Grant from the National Aeronautics and Space Administration

INTRODUCTION

In the past decade or so, considerable emphasis has been placed on the development of structural metals having high strength-to-density ratios. There has also been a continual search for stronger, tougher and cheaper alloys. In the attempt to maximize strength and satisfy the unusually high toughness requirements of today's designs, it is generally observed that, as the strength is increased, the toughness of a particular high-strength alloy usually drops off quite rapidly. Methods by which to attain high strength in 18 Ni maraging steels have been established and yet understanding of the physical metallurgy is limited. In order to strengthen this ductile material, plastic flow must be inhibited by intentionally introducing a dispersion of second phase particles by precipitation. Strengthening precipitates act as barriers to dislocation motion which in turn make the material resistant to plastic deformation. Although a material with high strength is realized, the material must simultaneously resist cracking in the presence of a crack or crack-like flaw. To avoid notch brittleness and potential catastrophic failure, any localized high stresses around both internal and external stress concentrators must be redistributed. This seemingly contradictory requirement imposes rather stringent conditions on the development of alloys that are simultaneously strong and tough.

Hence we can see why this leads to the frequent observation of strength varying inversely with toughness.

The purpose of this investigation is to systematically vary the strength of an 18 weight percent Ni, 300 grade maraging steel, isolate any attending microstructural changes and study the effects of these changes on the fracture toughness of this alloy. It is hoped that the work might satisfy the more general goal of whether or not there must be this continual trade-off between strength and toughness.

Work completed to date and reported herein includes:

1. Exploratory experiments performed to assess the magnitude of the decrease in toughness accompanying strength increases in a preliminary heat of maraging steel.
2. A metallographic investigation to define the nature of the non-metallic inclusion populations in the preliminary and program heats of steel.
3. Determination of the chemical composition and heat treating schedule for this alloy.
4. A fractographic study to characterize the fracture surfaces of the preliminary alloy at various strength levels.
5. A discussion of the current and future testing and proposed analyses.

MATERIALS

In order to choose a material which could be used to display recognizable trends between properties that appear to be as naturally opposing as strength and toughness, several criteria had to be satisfied. The design requirement of increased toughness without significant loss in strength is the goal of every materials user. The need for a sound understanding of the interrelationship of these properties is obvious.

Several investigations[1, 2, 3] have demonstrated that fracture occurs in most 18 Ni maraging steels by the plastic fracture process.[4] Plastic fracture is frequently referred to as dimpled rupture as a result of the microscopic appearance of the fracture surface. It has also been shown[1, 3, 5] that the nucleation of voids in high strength steels is caused by second-phase impurity particles, including sulfides, carbides and nitrides, depending upon the exact alloy.

To establish a viable experimental program, occurrence of a single mode of fracture over the entire range of strength considered would be desirable. In addition, since it is the strength property that we seek to systematically regulate, a material which can take on an extensive range of strengths would magnify the observable trend between strength and toughness and thus enhance the overall program. The alloy chosen should

also bear some resemblance to material which is commercially available. This is because the maximum toughness attainable has been shown to be a strong function of the exact nature of the second phase impurity inclusion particles and their spacial distribution and density.[5, 6] Highly segregated inclusions in an alloy would, for example, lead to a very specific relationship between strength and toughness instead of the general behavior characteristic of a more homogeneous microstructure. To this end, an 18 Ni, 300 grade maraging steel was chosen for preliminary evaluation. The 300 grade alloy was chosen since the literature[7] indicated that yield strengths ranging from approximately 110 to 300 ksi (758 to 2068 MN/m^2) could be realized through simple heat treatments. The somewhat more extensive range in strengths available in the age-hardenable 350 and 400 grades of maraging steel were not considered since fracture in these alloys has been shown to occur by an intergranular mode.[8] Evidence for plastic fracture of the 18 Ni, 300 grade maraging steel tested at room temperature at various strength levels in this study will be presented in subsequent sections.

Preliminary Alloy

The commercial 18 Ni, 300 grade maraging steel was provided in limited quantity for exploratory experiments. This material was from a seven-inch round bar rolled from a consumable electrode, vacuum remelted ingot. Additional information as to the exact size or processing history

of the heat was not available. The mill chemical analysis of the exploratory heat along with the chemical specifications for 300 grade maraging steel are given in Table I. Included in Table I is the analysis for the long-term program heat. The significance of the program heat will become apparent in the next section. It is noteworthy to compare the exploratory heat with the specifications for carbon, nickel, cobalt and titanium. The carbon is at one-tenth the maximum allowable, the cobalt level is at the rich end of the range, and the nickel and titanium levels are near the middle of their specified ranges.

It is important to the overall understanding of microstructural control that we consider the potential forms that carbon, sulfur, molybdenum, titanium and cobalt can take on. When maraging steels are examined by optical and electron microscopy, inclusions as well as precipitates are observed. As will become more apparent as we go on, molybdenum, titanium and cobalt are intentional additions which, it is hoped, will preferentially interact in solid-state precipitation reactions during aging treatments to form strengthening precipitates. While precipitates are the entity which when interacted with dislocations in the matrix provide the desired strength, the inclusions can be detrimental to toughness and hence are undesirable.[9] Titanium is an element which has a high affinity for carbon. Along with the similar potential of molybdenum to combine with carbon, the resulting

TABLE I

CHEMICAL ANALYSES OF 300 GRADE,
18 Ni-Co-Mo-Ti MARAGING STEELS
(Weight Percent)

	Commercial Specification	Exploratory Heat Mill Analysis	Program Heat Mill Analysis	Program Check Analysis*
C	0.03 Max	0.003	0.003	0.002 ± 0.002
Mn	0.10 Max	0.05	0.02	0.04 ± 0.01
Si	0.10 Max	0.01	0.01	0.03 ± 0.01
S	0.010 Max	0.005	0.006	0.005 ± 0.001
P	0.010 Max	0.006	0.001	0.005 ± 0.001
Ni	18.0/19.0	18.27	18.29	18.53 ± 0.01
Mo	4.6/5.2	4.97	4.93	4.77 ± 0.05
Co	8.5/9.5	9.50	8.98	8.63 ± 0.1
Al	0.05/0.15	0.13	0.10	0.12 ± 0.002
Ti	0.5/0.8	0.68	0.63	0.65 ± 0.01
Zr	0.02 Added	0.010	0.016	0.015 ± 0.001
B	0.003 Added	0.003	<0.001	<0.001 ± 0.001
Ca	0.05 Added	0.05 Added	-	0.025 ± 0.01
N_2	-	-	-	0.005 ± 0.001
Fe	Balance	Balance	Balance	Balance

*Average from two separate test blocks.

formation of impurity particles while in the melt prevents the embrittlement of grain boundries by titanium carbide networks at prior austenite grain boundaries which might otherwise be more detrimental to ductility. Sulfur as well as carbon will tie up large amounts of titanium in the form of inclusions. The loss of titanium into the inclusions would prevent the realization of the full strength of the steel due to a reduction in the number of strengthening precipitates that could form.[9] Second-phase impurity inclusions have been shown to be the weak link leading to void formation and subsequent dimpled rupture.[3,10] The second-phase impurity inclusions are formed while the steel is liquid and cannot be removed or altered in the solid state by aging or other such thermal treatments.

Optical microscopy of polished sections of the exploratory heat has revealed inclusions of at least two different morphologies. The claim for different types of inclusions is based solely on appearance as observed under white light and distinguished with respect to their color, size and particularly, shape. Comparisons have been made with inclusions cited in the literature.[9] Metallographic sections from the round bar exploratory alloy were examined from each of three orthogonal directions, the axes being defined by the rolling, the radial and the circumferential directions. Figure 1 presents typical examples of the most prevalent inclusion types in this 18 Ni, 300 grade maraging alloy. As characterized by shape, at least two types can be distinguished. The square-like particles appeared as sections of cubes and

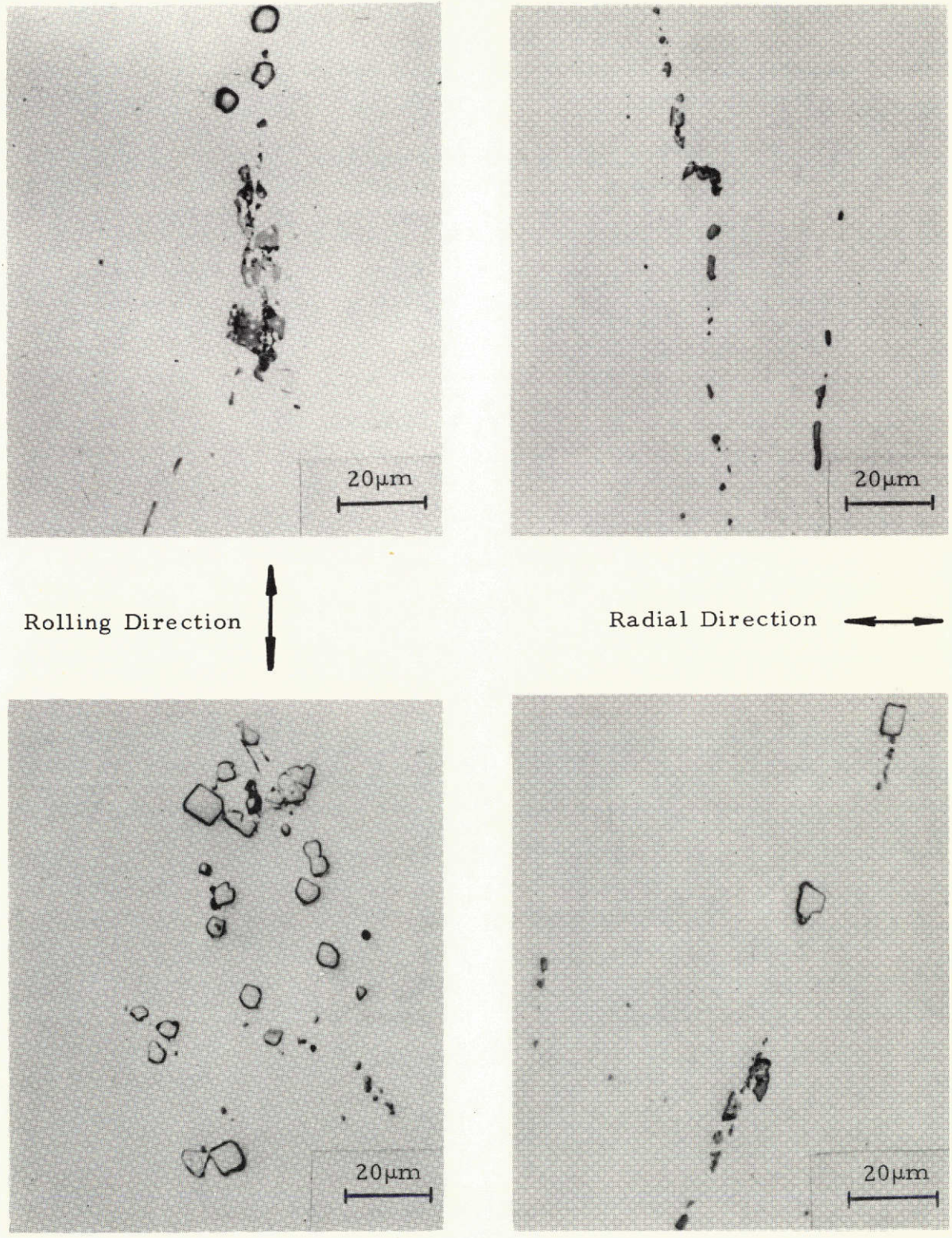

Figure 1 Optical micrographs of the most prevalent inclusions in the exploratory heat of 18 Ni, 300 grade maraging steel.

exhibited a pink or orange color in the optical microscope. In selected instances, the cubes appeared unsymmetric and rounded. In general, however, the cubic sections seemed to have approximately the same size distribution in each of the three views and did not appear to have been plastically deformed during the hot rolling operation. The other inclusions appeared elongated, broken up and highly irregular in shape. This second type of inclusion appeared dove gray, with a slight mauve or violet tinge. The irregular inclusions appear to have acquired their shape as a result of deformation during the mechanical working of the steel. Some inclusions have evidently cracked during rolling. Photographically, the color difference between the two inclusion types is difficult to discern but direct optical examination reveals distinct pink versus gray. In addition, in some cases the pink and gray inclusions are in contact with one another. Comparison of these optical metallographic observations with those of previous investigations,[9,11] led to a preliminary identification of the cubic inclusions as titanium carbonitrides (Ti(C, N)) and the irregular inclusions as titanium sulfides (Ti_2S). Had this been the long-term program alloy, a detailed quantitative analysis would have been performed to clearly identify these inclusions.

As might be expected, homogeneity of microstructure should influence the toughness attainable at a given strength level. Figure 1 clearly indicates

that the inclusions are highly clustered. Fractographic evidence for clustering will be presented in a subsequent section of this report. Inclusions frequently run in stringers. In addition, the exploratory heat has groups of inclusions which are often crowded together. In having the inclusions so closely grouped, link up into a massive void can occur shortly after the discrete inclusions have formed voids. Inclusion size is also a key factor for void initiation in plastic fracture.[3, 12] The clustering was later traced in part to an inadequate calcium deoxidation practice in the melt.[13] When the sulfur can be made to preferentially combine with calcium in the melt, the overall sulfur gettering action of titanium can be controlled and, in turn, can result in a reduced susceptibility for clustering. There has also been an observed tendency for molybdenum and titanium to segregate during solidification,[14] which might contribute to this problem. A more homogeneous starting material was considered better to approach the goals of the overall program. Materials from several sources were studied.

Program Alloy

The commercial purity 18 Ni, 300 grade maraging steel chosen for the long term program was made as a regular mill production heat. The heat was originally vacuum induction melted, cast into a 21-inch round

electrode and subsequently vacuum arc remelted into a 25-inch diameter ingot. Hot working of the ingot was accomplished in two steps, the first of which involved press forging the ingot to a plate 15 inches wide by 3.5 inches thick using a starting temperature of 2100°F (1149°C). After surface conditioning, the material was hammer forged using a starting temperature of 2100°F (1149°C) to a bar 10.5 inches wide by 2.3 inches thick. The bar was then annealed at 1500°F (815.5°C) and machined to the as-received dimensions of slightly over 10 inches wide by 2 inches thick. Annealing left the plate in the soft Rockwell "C" 30 hardness condition. The chemical specifications, heat and check analyses are shown in Table I.

The as-received plate was sectioned through the thickness in two locations, deep etched and found to be macroscopically sound. A uniform forging deformation flow pattern was revealed by etching in a HCl-HNO_3-H_2O solution mixed in the ratio of 1:1:2.

Typical optical micrographs of polished and etched sections of the program alloy are presented in Figure 2. The 18 Ni, 300 grade maraging steel is etched in Kalling's reagent, $CuCl_2$ and HCl in methanol and H_2O. This alloy exhibits very fine martensite laths shown in Figure 2. The prior austenite grain boundaries can be more clearly delineated by suitable etchants. The micrographs shown in Figure 2 were taken from specimens aged for 3 hours at 900°F (482.2°C). A well-developed Widmanstatten-like morphology is evident. Floreen and Decker

Longitudinal
(Forging)
Direction

Transverse
Direction

Figure 2 Optical micrographs of typical areas from polished and etched sections of the program heat of 18 Ni, 300 grade maraging steel.

attribute the Widmanstatten-like structure to the martensitic transformation occurring upon cooling from the annealing temperature of 1500°F (815.5°C).[15] While at the annealing temperature, the structure is austenitic, face-centered cubic. The structure as shown in Figure 2 is apparently entirely body-centered cubic martensite. Little, if any, of the body-centered cubic phase should have reverted to austenite during the short time at 900°F (482.2°C). Uniform hardness and chemical composition is expected across sections of dark and light platelets.[15] Subsequent microprobe work will be performed on the program heat to confirm the uniformity of composition across these platelets. The etched sections provide some evidence for the presence of non-metallic inclusions; however, the etching has obscured them to some extent. Much of the fine detail of the inclusions and their orientation with respect to the martensite laths will be examined with surface replication techniques. The replicas of the polished and etched sections will be observed in the transmission electron microscope.

Polished metallographic sections were examined from each of three orthogonal directions in the program heat of maraging steel. The axes were defined using ASTM E399-72 terminology as the length, L (the major forging direction in this case), long transverse, T (the width) and the short transverse, S (the through thickness). As in the exploratory

heat, at least two types of second-phase impurity inclusions are present. Preliminary identification was made based upon size, shape and color as described earlier for the exploratory work. The most prevalent shapes are shown in Figure 3. Those appearing as sections from cubes and sometimes rounded are pink in color and are believed to be titanium carbonitrides (Ti(C, N)). As shown in Figure 3, the two types of inclusions are often in contact with one another. Some of the cubic inclusions showed central black dots similar to those reported in the literature which were shown to contain zirconium.[9] The zirconium present in the center of Ti(C, N) may be either in the form of zirconia or zirconium carbonitride. It has been suggested that since both zirconia and zirconium carbonitride have very high melting points, these may be the first to solidify from the melt and provide a nucleus for growth of the Ti(C, N).[16] The light gray elongated and irregular inclusions are compared to titanium sulfides (Ti_2S) and titanium carbides (TiC) observed in a previous investigation.[9] To ascertain whether or not this tentative identification of the non-metallic inclusions is correct, specimens will be examined by using a scanning electron microscope equipped with an X-ray energy-dispersive analyzer.

As expected, this heat has inclusions which tend to conform to the major hot working direction. Some of the inclusions have cracked,

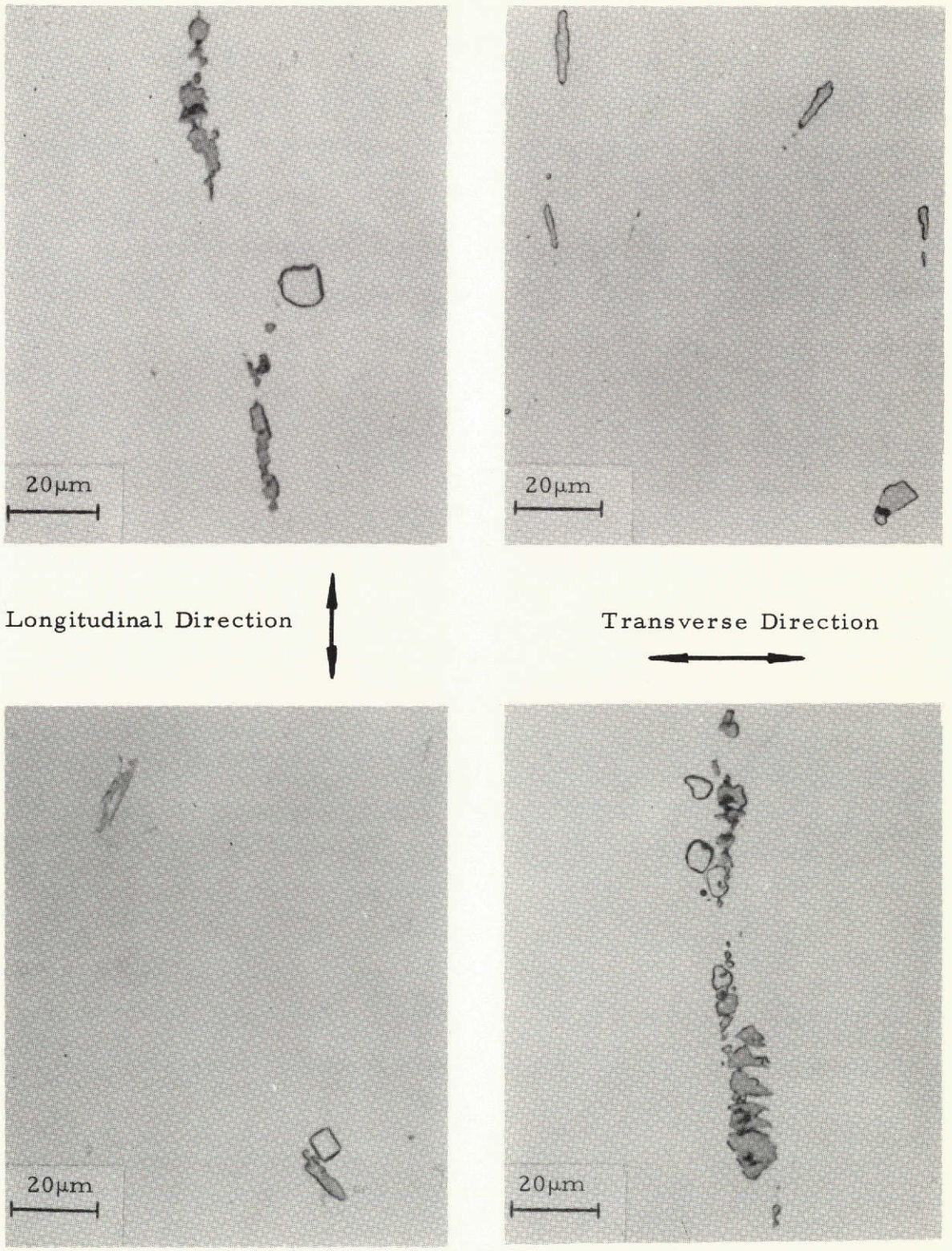

Figure 3 Optical micrographs of the most prevalent inclusions in the program heat of 18 Ni, 300 grade maraging steel.

presumably due to the mechanical working. It is not entirely clear at this time whether both inclusion types have cracked. Care must be taken when identifying the black areas in Figure 3 as cracks since some of these may be another phase within the inclusion. The degree of inclusion clustering has been reduced considerably and the average inclusion size reduced. This observation may not be readily apparent from Figure 3 since these examples were intended primarily for characterization of the inclusions. In the preliminary alloy, inclusions were frequently as large as 10 microns (μm) in one or more dimensions, as revealed optically. The program alloy, as typically shown in Figure 3, contains inclusions which are usually less than 10 μm in diameter. It should be noted that although both heats contain a distribution of inclusion sizes ranging from less than 1 μm to approximately 10 μm, the program heat has the cuboidal inclusions more homogeneously distributed throughout the matrix. Optical microscopy alone cannot reveal the smallest inclusions in this distribution which tend to be uniformly dispersed throughout the matrix. It will become more apparent later in this report that inclusion size may be a key variable controlling toughness. A quantitative metallographic investigation is planned to determine the exact nature of the inclusion populations as to types, sizes, shapes and distributions.

AGING STUDY

To complement the exploratory investigations, a study aimed at determining the aging behavior of the program alloy was carried out. Since material will be aged at various temperatures to arrive at specified strength levels, it is important to know the extent of hardening and the kinetics of the age-hardening process as a function of both time and temperature. This would require data generated isothermally (constant temperature of aging, varied time) as well as isochronally (constant time at temperature). Since several temperatures are to be used, isothermal data can be used to draw isochronal curves. Such a study is justified since the plan is to test the toughness of the 300 grade maraging steel at various strength levels. Small variations in composition about the specification with respect to molybdenum, titanium and cobalt, when considered as to their solid-state interactions, can significantly vary the hardness attainable in various heats of maraging steel subject to the same thermal treatments.[17,18] Ultimately, strength and plane-strain fracture toughness will in part be characterized respectively by tension tests and by compact tension and slow-bend K_{Ic} specimens. An aging study can provide data by which to estimate yield strength. When used in conjunction with estimates of toughness at that same strength level, the specimen

thickness requirment for valid plane-strain fracture toughness can be predicted.[19, 20] Methods of estimating toughness will be discussed in a following section of this report.

The plan is to study the plane-strain fracture toughness of this 300 grade maraging steel as a function of strength ranging from about 160 to 300 ksi (1102 to 2068 MN/m^2). This will include the underaged, peak aged and overaged conditions. Originally it was planned to perform isochronal aging treatments of 3 hours at temperatures of 500, 700, 800, 900 and 1000°F (260, 371.1, 426.7, 482.2 and 537.8°C). Since the maraging plate limits toughness specimens to two-inch thickness, the low strength produced by aging for 3 hours at 500°F (260°C) cannot be validly tested. Toughness specimens as thick as four inches would be required. This can be seen by considering the empirical relation, $B = 2.5 (K_{Ic}/\sigma_{ys})^2$ proposed by Brown and co-workers.[19, 20] As σ_{ys}, the yield strength, is decreased, the specimen thickness, B, must be increased to satisfy this relationship.

In support of valid toughness testing, a detailed isothermal aging study to record the kinetics of the maraging hardening process in the program heat is in progress. Hardness blanks of 0.25 inch thickness are being isothermally aged at 600, 650, 700, 800, 900 and 1000°F (315.5, 343.5, 371.1, 426.7, 482.2 and 537.8°C). Aging treatments are being

performed in air to parallel the heat treatment procedure necessary for aging toughness specimens which are as large as 17 inches long by 4 inches wide in the 2-inch thick case. A plot of Rockwell "C" hardness versus time at temperature is presented in Figure 4 for 600°F (315.5°C), 650°F (343.5°C) and 1000°F (537.8°C) aging temperatures. Each datum point is the average of five hardness indentations per test block. The ultimate plan is to use 3-hour isochronal aging treatments to attain various strengths in the relatively thick section toughness specimens. The choice of low temperature (low strength) must satisfy the plate thickness limitation for toughness specimen design. The 600 and 650°F (315.5 and 343.5°C) aging temperatures have been employed to determine the proper treatment for subsequent investigation. After nearly 500 hours at temperature, these low temperature curves in Figure 4 have not yet reached peak hardness. The kinetics of hardening at 1000°F (537.8°C) are such that peak hardness is reached after approximately 2 hours at temperature for this heat of steel. Loss of hardness (strength) due to overaging is expected to be due primarily to a time-dependent reversion of the metastable body-centered cubic martensite to the equilibrium face-centered cubic austenite.[21]

In addition to simply determining the proper set of aging temperatures to use in this study, the variously aged blocks of material can be subsequently observed via thin foil transmission electron microscopy to

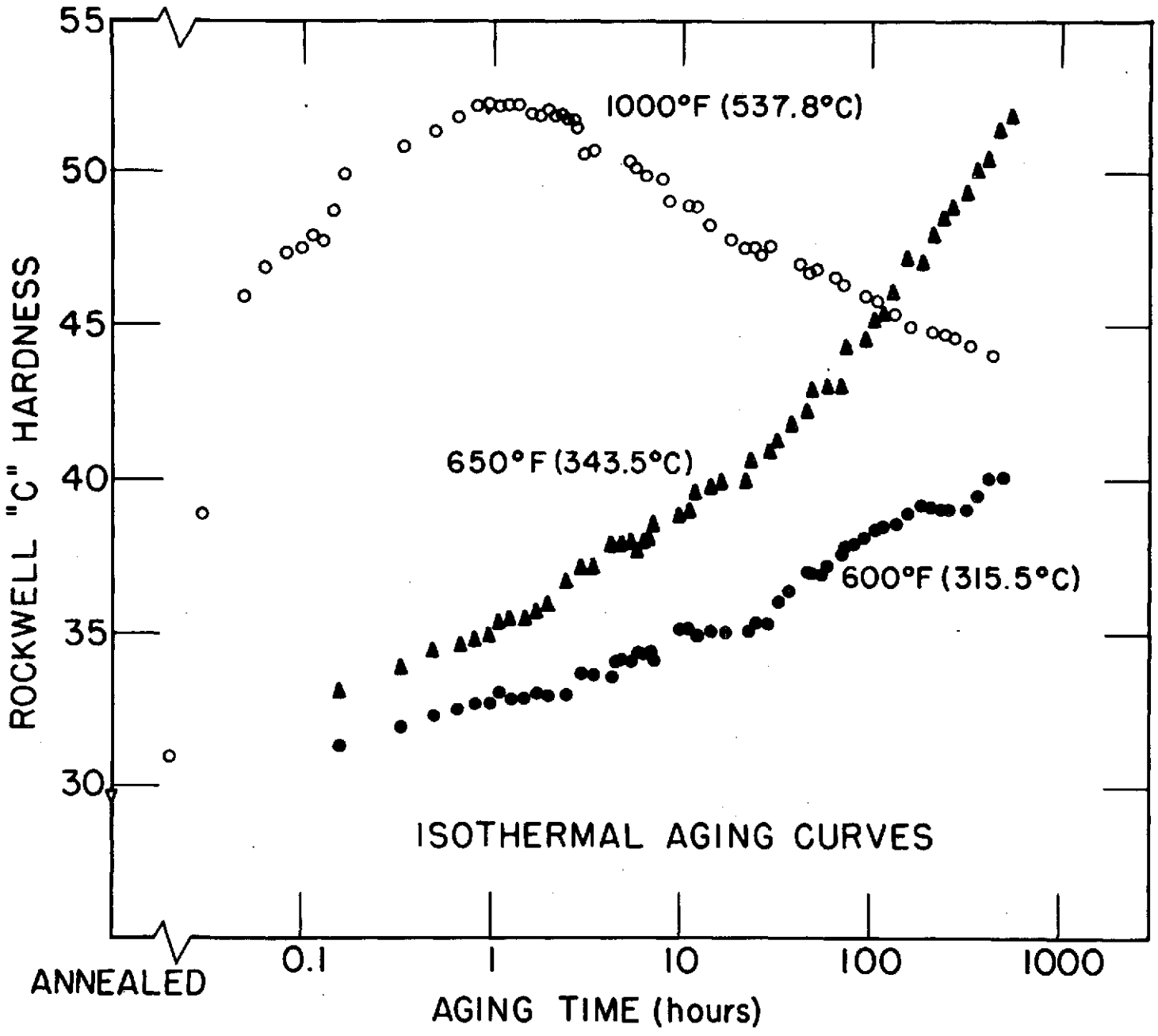

Figure 4 Hardness versus logarithm of time at temperature for some of the aging treatments to be used on the program heat of 18 Ni, 300 grade maraging steel.

examine the growth of strengthening precipitates. Through such observations, one must determine if there are any compositional and/or structural changes in the strengthening precipitates as time at temperature increases. This is important to consider since precipitates are often purposely overaged to aid in their identification by diffraction methods. The grossly overaged precipitate may not in fact be the same precipitate as was present in the earlier stages of growth due to structural transformations. Peters[22] has reported evidence for two types of molybdenum-rich precipitates in 18 Ni, 250 maraging steel, one nucleated at dislocations and the other in the matrix. The matrix precipitate is dominate when aging is for short times at temperatures below 850°F (455°C). Above this temperature, the frequently observed dislocation-nucleated precipitate is dominate.

The fine internal structures of 18 Ni maraging steels have been studied by many previous investigations.[15, 17, 21] Until the work of Spitzig, Chilton and Barton[23] in 1968, only very limited data was available as to the strengthening entities in 18 Ni, 300 grade maraging steels. In these previous investigations, the strengthening precipitates were identified by means of extraction replication techniques as Ni_3Mo, and possibly Ni_3Ti. In this more recent work,[23] precipitates were identified through selected-area electron-diffraction. Two different precipitates were found within the martensite laths. These precipitates were

identified as an orthorhombic Ni_3Mo phase and a tetragonal phase. Diffraction patterns from this tetragonal σ-phase were not consistent with Ni_3Ti, Fe_2Ti, cubic FeTi or any of the other possibilities that have been suggested in previous investigations of 250 grade maraging steel.[24] In accordance with their previous work,[24] the tetragonal phase was designated as σ-FeTi. They also noted that the sigma phase might be different from FeTi (for example, CoTi, NiTi) because the lattice parameters of all sigma phases are similar.

Subject to an even greater controversy is the role of cobalt in strengthening maraging steels. Two schools of thought are evident. Some suggest that cobalt might decrease the solubility of Mo in the Fe-Ni martensite, resulting in a more copious nucleation and hence more finely dispersed Ni_3Mo precipitates leading to greater strength.[21] Others[17] argue that the effect of cobalt on matrix strengthening is based on cobalt lowering the stacking-fault energy of the matrix. Since the stacking-fault argument applied to the material while in the austenitic condition, the authors appeal to dislocation cell size measurements in the body-centered cubic martensitic condition for support of their argument. They propose that cell size and twin density are observable parameters in the body-centered cubic structure that significantly depend upon the stacking-fault energy. The claim is essentially that the lowered stacking-fault energy would discourage cross-slip and retard cell growth. The resulting

increase in average dislocation density provides more nucleation sites for the precipitates which stabilize the dislocation forest and increase interference for moving dislocations; thus, strength is apparently improved in the aged condition. Although most investigators have observed two distinct precipitates, there is still some discussion as to the exact nature of these phases. At present the exact role of cobalt, which does not enter significantly into any of the precipitates but provides added strength to the matrix, is at best confused.

For many years, toughness was believed to be solely associated with dislocation interactions with the strengthening precipitate Ni_3Mo.[18] The recent works of Roesch and Henry[1] and particularly of Cox and Low[3] show the importance of second-phase impurity inclusions on the plastic fracture process and, in turn, the fracture toughness property. Through thin foil transmission electron microscopy, the growth of strengthening precipitates and changing dislocation morphology resulting from aging should provide a link between matrix strength and toughness. A sound understanding of how the matrix strength and flow properties change with degree of aging is necessary to arrive at the ultimate link between resistance to deformation and susceptibility for cracking in high-strength materials such as the 300 grade maraging steels.

MECHANICAL TESTING

The mechanical properties of the 300 grade maraging steel will be characterized using tension tests, fatigue precracked Charpy impact tests and plane strain fracture toughness tests.

The first step was to ascertain whether or not the expected trend for decreasing toughness with increasing strength was extensive. The experimental program used fatigue precracked Charpy specimens machined from the seven-inch round exploratory alloy in the CL orientation (major Charpy specimen axis in the circumferential direction and the crack path in the longitudinal direction). Although this orientation would not normally be desired, it was used in the preliminary tests due to material limitations. The Charpy bars were precracked in fatigue so as to sharpen the crack and provide data that could more reasonably estimate the fracture toughness.[25] The exploratory heat was supplied in the solution annealed condition with Rockwell "C" hardness 31.0 and roughly 110 ksi (758 MN/m^2) yield strength. Duplicate Charpy specimens were aged at each of five aging temperatures: 500, 700, 800, 900 and 1000°F (260, 371.1, 426.7, 482.2 and 537.8°C). Standard aging treatments were 3 hours at temperature followed by air cooling. Corresponding yield strengths estimated from hardness data in the literature[7] were: 142, 175, 242, 290 and 255 ksi (979, 1207, 1669, 1999 and 1758 MN/m^2). The

drop in strength to 255 ksi (1758 MN/m^2) for the 1000°F (537.8°C) aging treatment is a result of the overaged condition. Charpy data are given in energy loss per unit uncracked area based on an average of two tests per strength level. Room temperature impact test results listed in Table II show a significant inverse relationship between strength and toughness. It is important to note that the estimated toughness data represent a decrease in toughness of approximately 116 ksi/in (127.6 $MNm^{-3/2}$) for a strength increase in the material of 148 ksi (1020 MN/m^2) in going from the 500°F (260°C) age to the peak strength age at 900°F (482.2°C). Also note that there has been no claim that these toughness data satisfy the criteria as outlined in ASTM standard E399-72 for valid K_{Ic} measurements.[26] The data are estimates of K_{Ic} determined from the fatigue precracked Charpy impact tests and correlated to K_{Ic} through the total energy per unit area, W/A, involved in fracture.[25] When these estimated toughness versus estimated yield strength data are plotted in Figure 5, the extremely sharp trend is evident. On the basis of these data, we can conclude that there is a significant inverse relationship between strength and toughness.

At the estimated 142 ksi (979 MN/m^2) strength and 177 ksi/in (194.7 $MNm^{-3/2}$) toughness level, the 500°F (260°C) aged condition would require 4-inch thick K_{Ic} specimens to satisfy the thickness

TABLE II

MECHANICAL TEST RESULTS: TOUGHNESS-PRECRACKED CHARPY
300 GRADE MARAGING STEEL

Aging Temperature °F (°C)	Rockwell "C" Hardness	Yield Strength (ksi) Estimated from Hardness (1 ksi = 6.89 MN/m^2)	Energy Absorbed per Unit Uncracked Area in Impact (in-ℓb/in^2) (1 in-ℓb/in^2 = 175 Nm/m^2)	Estimated[22] K_{Ic} (ksi$\sqrt{in}$) (1 ksi$\sqrt{in}$ = 1.10 $MNm^{-3/2}$)
500 (260)	33.5	142	1892	177
700 (371.1)	43.0	175	960	126
800 (426.7)	50.0	242	280	68
900 (482.2)	54.5	290	227	61
1000 (537.8)	53.0	255	285	69

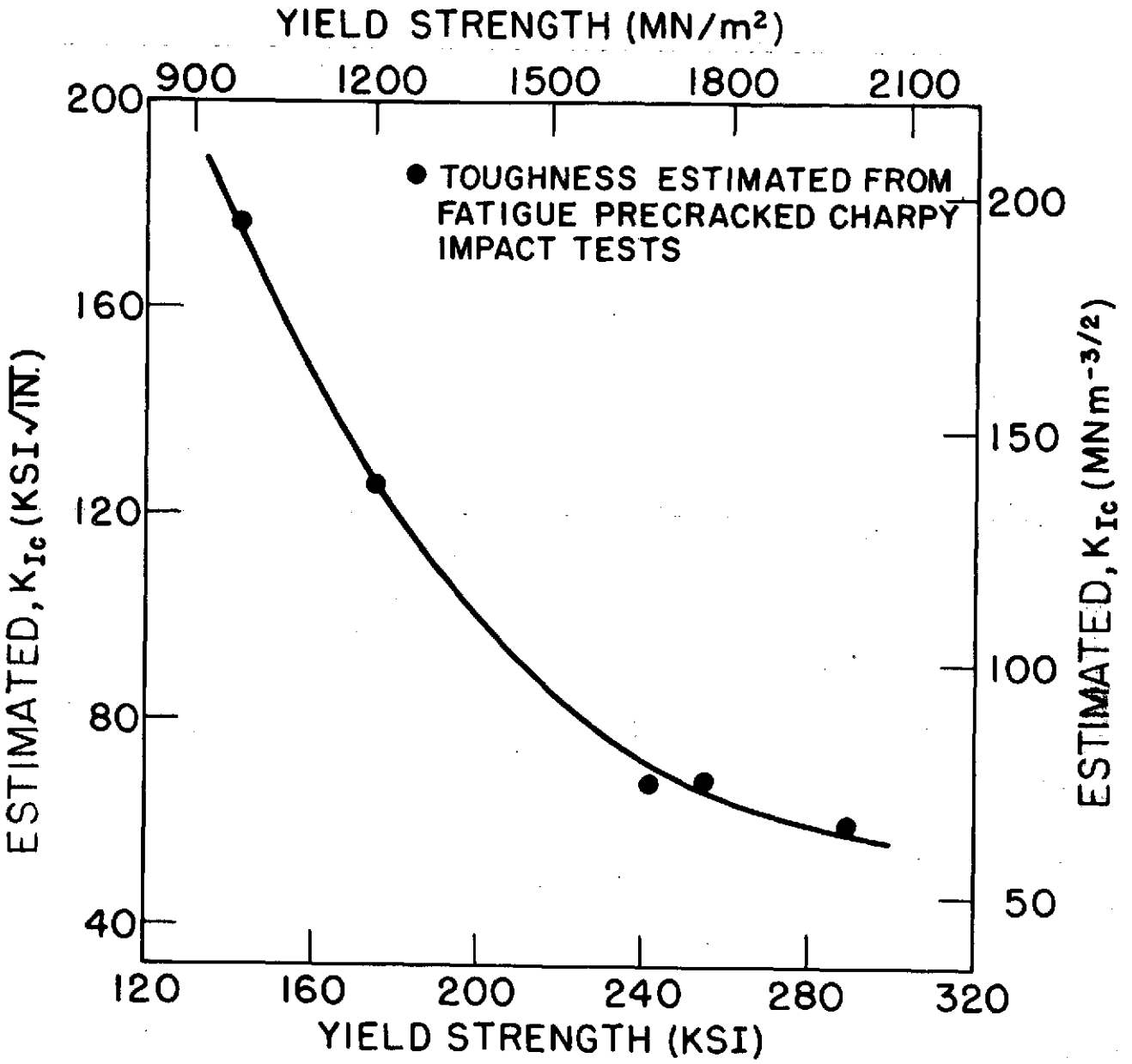

Figure 5 Plane strain fracture toughness data estimated from room temperature fatigue precracked Charpy impact tests of the variously strengthened exploratory heat of 300 grade maraging steel.

requirements for valid toughness testing. The program heat of 300 maraging steel was available as 2-inch thick forged plate. An aging analysis is now being performed concurrent to mechanical test specimen machining. Aging temperatures will include: 600, 700, 800, 900 and 1000°F (315.5, 371.1, 426.7, 482.2 and 537.8°C). The only temperature in question is 600°F (315.5°C), which may have to be increased slightly so that slightly higher strength and corresponding lower toughness can yield valid toughness data. The 300 grade maraging steel in the 600°F (315.5°C) and 700°F (371.1°C) aged conditions will be tested as 2-inch thick, three-point bend K_{Ic} specimens. All tests will be performed at room temperature (70°F). The 2-inch thick K_{Ic} tests will be performed at NASA Lewis Research Center. All of the other (higher) strength levels to be tested in our laboratory will use 0.75-inch thick compact tension specimens. Both facilities meet the requirements of the ASTM standard for fracture toughness testing.[26]

The mechanical testing of the program alloy will begin with a similar but more detailed estimation of toughness as a function of strength with fatigue precracked Charpy samples. The Charpy samples will be held in a three-point bend fixture and fatigued while in the strength condition in which they are to be tested in impact. The mechanical testing would also include standard 0.252-inch diameter tension specimens

at all levels of aging to evaluate strength and material flow properties. Since dimpled rupture appears to be the controlling mode of fracture, the tentative plan is to use tension specimens to relate the void initiation, growth and coalescence stages of plastic fracture to the crack initiation and propagation in the K_{Ic} specimens. In addition, precracked Charpy, K_{Ic} and tensile fracture surfaces will be compared to better characterize the fracture mechanism. Should fractographic evidence indicate that the K_{Ic} and tensile fractures are statistically identical, variously strained and sectioned tensile specimens could then provide one means to isolate the microstructural features controlling plastic fracture. Fractography as a technique provides a unique approach to viewing key features evident in the topography of the fracture surface. When these techniques are used in conjunction, the observations are complementary to the complete understanding of the mechanism of plastic fracture.

FRACTOGRAPHY

A fractographic study was carried out on the exploratory heat of 18 Ni, 300 grade maraging steel to assess the nature of the fracture surfaces relative to their strength levels. It should be made clear that we are studying the fracture response of precracked Charpy specimens taken from a single material and tested in impact at various levels of matrix strength. Two stage, cellulose acetate-platinum shadowed carbon replicas were taken from the areas of fast fracture initiation on the fatigue precracked Charpy fracture surfaces. The replicas were examined in the electron microscope. Fractographs will be referred to by the aging temperature of the specimen from which they originate. The strengths follow the trend reported in Table II.

Typical fractographs of the room temperature impact fracture surfaces of the 500, 700, 800, 900 and 1000°F (260, 371.1, 426.7, 482.2 and 537.8°C) aged Charpy specimens are presented in Figures 6 through 10, respectively.

Examination of the 18 Ni, 300 grade maraging fractographs in Figures 6 through 10 reveals that the fracture mode was dimpled rupture at all strength levels observed for the Charpy specimens broken at room temperature. Dimpled rupture is the mode of fracture whereby microscopic voids nucleate at second-phase particles, then grow and coalesce

to cause final rupture. At the lowest strength level considered, Figure 6 shows the fracture surface to be almost completely covered by only large dimples approximately 15-20 μm in diameter. At the positions marked "X" on the fractograph, examples of impressions of what have been tentatively identified as titanium carbonitride inclusions may be seen at the bottom of dimples. The position marked "Y" appears to be associated with the irregular inclusions alluded to earlier. There is evidence for inclusion shattering at all strength levels as shown, for example, at position "Z" in Figure 6. When the fractographs were viewed as stereo pairs, the dished out material (dimple) appears to have been nucleated by the separation of the halves of the fractured inclusions.

With increasing strength (Figure 7), two populations of dimple sizes were observed (1-5 μm and 5-15 μm in diameter), presumably resulting from failure of a broader range of inclusion sizes from the entire population of inclusions present in the material. One might expect the average dimple size to decrease since more void nucleation sites are active and, hence, less void growth between neighbor voids is necessary before gross separation of the material. Figure 7, the 700°F (371.1°C) aged Charpy, reveals these features with the large dimples in the upper right portion of the fractograph. The smaller dimples to the left and bottom appear to surround the large dimples. Other observations at this strength level

(Tentatively identified titanium carbonitrides indicated by X; irregular shaped inclusions indicated by Y; shattered inclusions indicated by Z)

Figure 6 Electron fractograph from the fatigue precracked Charpy fracture of the exploratory 18 Ni maraging steel aged at 500°F (260°C) and tested at room temperature.

(Large inclusions and associated large dimples indicated by X; small inclusions and associated small dimples indicated by Y)

Figure 7 Electron fractograph from the fatigue precracked Charpy fracture of the exploratory 18 Ni maraging steel aged at 700°F (371.1°C) and tested at room temperature.

(not shown) are suggestive of the clustering problem in the exploratory heat in that a band of large inclusion nucleated dimples will frequently be surrounded by smaller dimples similar to those shown in Figure 7. Again, the important feature changes to note in Figure 7, not evident at the lower strength level of Figure 6, are the large and small inclusions and associated dimples marked "X" and "Y", respectively.

The substantial increase in strength from approximately 175 ksi (1207 MN/m^2) to 242 ksi (1669 MN/m^2) associated with the increase in aging temperature from 700°F (371.1°C) to 800°F (426.7°C) has resulted in extensive changes in the fracture appearance of this same exploratory alloy. In the 800°F (426.7°C) fractograph shown in Figure 8, the average dimple size is smaller. The larger dimples range from 5 to 10 μm in diameter, and the finer dimples are 1 or 2 μm in diameter or less. All of the large inclusions which were present in both of the lesser strength conditions seen thus far are active in the 800°F (426.7°C) aged Charpy fracture. In addition, as seen in regions marked "A", there are finer markings which appear to be grouped in colonies and made up of a large number of small open-ended dimples. The exact mechanism by which these fine dimples form is not understood at this time. The dimples in the 800°F (426.7°C) aged condition appear much shallower than in either of the lower strength conditions seen in Figures 6 and 7. Since the magnifications are identical

(Regions with many fine dimples marked A)

Figure 8 Electron fractograph from the fatigue precracked Charpy fracture of the exploratory 18 Ni maraging steel aged at 800°F (426.7°C) and tested at room temperature.

in Figures 6 through 10, the increased number of dimples per unit of fracture surface is evident as the strength is systematically increased. That is to say, the dimple size is decreasing. These crude approximations must be subsequently supported by quantitative statistical measurements from many representative fractographs. Although some impressions of fractured inclusions resemble the elongated and irregular gray particle seen optically, the more generally observed inclusion is the angular carbonitride. To draw inference as to the importance of either inclusion type at this point in the investigation would be entirely speculative in nature.

When viewed stereographically, the topography of the fracture surfaces become increasingly more rugged with abrupt level change between adjacent features as the peak strength in the 900°F (482.2°C) aged condition is approached. At the 142 ksi (979 MN/m^2) strength condition, the features are rounded and the greater ductility is reflected by the very deep dimples associated with this condition. At the 242 ksi (1669 MN/m^2) strength level (800°F (426.7°C)) and above, large patches of shallow dimples (Figure 8) are noted. Sharp level changes are a key feature of Figure 9. Although best seen in the stereo pairs, the area which is analogous to a ledge is marked "X" in Figure 9. In this, the fully aged, 300 ksi condition, dimples greater than 5 to 10 μm are

(Area analogous to a ledge with a dense population of what appear to be submicron dimples indicated by X)

Figure 9 Electron fractograph from the fatigue precracked Charpy fracture of the exploratory 18 Ni maraging steel aged at 900°F (482.2°C) and tested at room temperature.

infrequent and typically dimples are now from 1 to 5 μm in diameter. Although the same inclusions are present in the matrix at this strength level, apparently inclusions of an even more extensive size range are contributing to the fracture. Much of the ledge feature of Figure 9 is covered by craze-like markings. Close observation of these features suggests that these might be very fine dimples associated with submircon sized particles. The possibility that these particles might be the strengthening precipitates has been suggested.[1] The evidence at this time is too sketchy to be more definitive about the exact mechanism of fracture. Figure 10 is from the 1000°F (537.8°C) aged Charpy broken at room temperature. This fractograph shows the reduction in strength in that the large dimples appear in the range of 5 to 10 μm. There are, however, many smaller dimples associated with the finer inclusions and ledge-like areas of submicron dimples similar in appearance but of lesser volume than the 900°F (482.2°C) condition. Evidence for reverted austenite in the overaged condition could not be either supported or refuted on the basis of this brief examination.

One goal of the exploratory work was to find a single alloy which could display an extensive range in strength. To this end, low temperature testing was considered since the 300 grade maraging would have a higher yield strength when tested at liquid nitrogen rather than at room

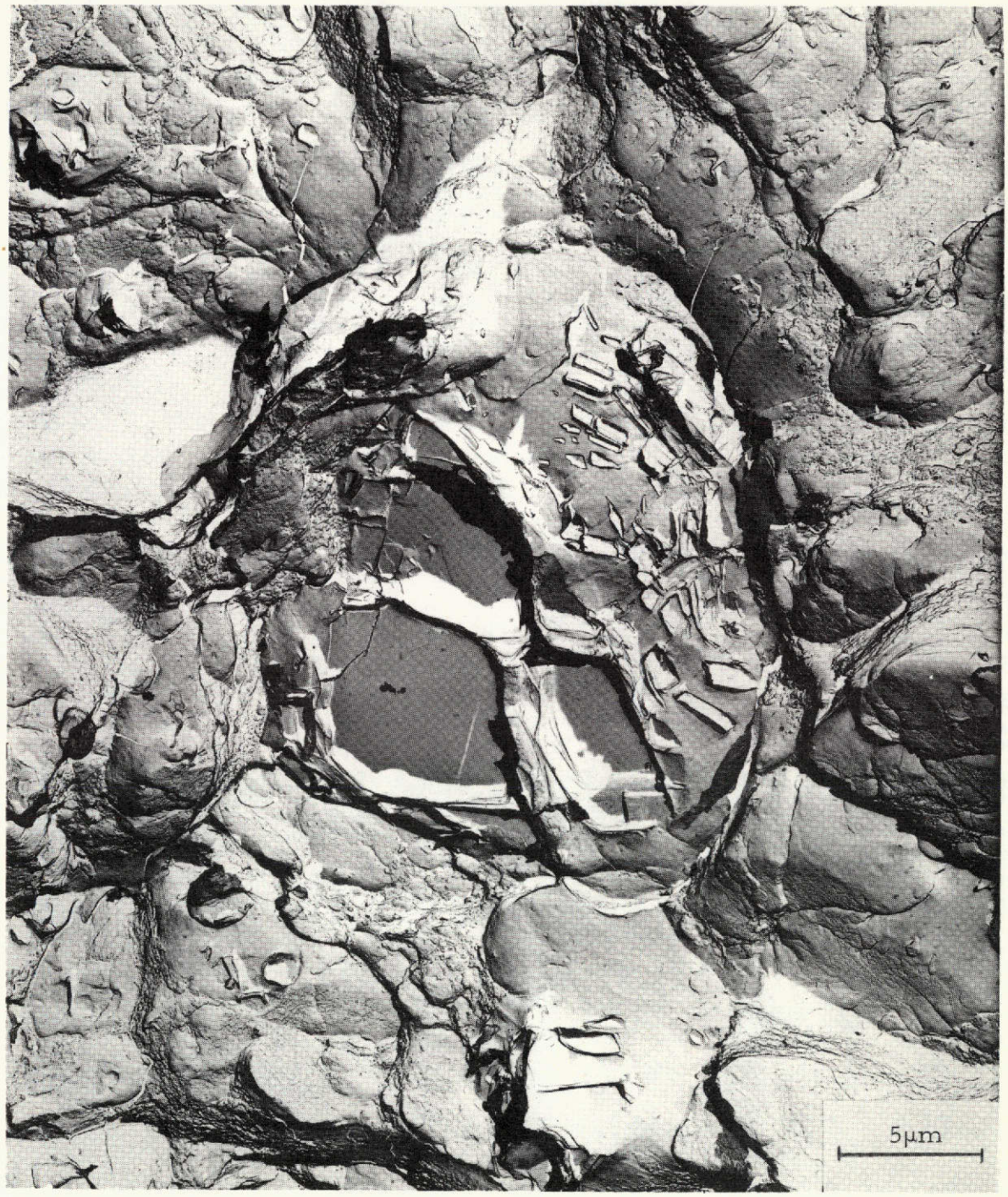

Figure 10 Electron fractograph from the fatigue precracked Charpy fracture of the exploratory 18 Ni maraging steel aged at 1000°F (537.8°C) and tested at room temperature.

temperature. To test the response, a 900°F (482.2°C) fully aged pre-cracked Charpy was tested at -320°F (-196°C). Typically (Figure 11), the fracture surface was a mixture of dimples and sharply stepped areas. The inclusions were either obscured in the fracture or generally not present, which would suggest that the mode of fracture did not require inclusions as a weak link. Figure 12 shows an infrequent, yet interesting, occurrence in the liquid nitrogen fracture. The river patterns are suggestive, yet not conclusive, evidence of cleavage fracture in this select region. The cleavage facet shown in Figure 12 is approximately 30 to 35 μm across. Although the grain size of the exploratory heat was not determined, this structural feature is comparable to a fine prior austenite grain size expected for this heat of steel.

Figure 11 Electron fractograph from the fatigue precracked Charpy fracture of the exploratory 18 Ni maraging steel aged at 900°F (482.2°C) and tested at liquid nitrogen temperature.

Figure 12 Electron fractograph from the fatigue precracked Charpy fracture of the exploratory 18 Ni maraging steel aged at 900°F (482.2°C) and tested at liquid nitrogen temperature.

DISCUSSION

It has been demonstrated above in the exploratory heat of 18 Ni, 300 grade maraging steel that the trend in fracture toughness as estimated by fatigue precracked Charpy data is indicative of a significant inverse relationship between strength and toughness. Apparent trends in fractographic evidence suggest some parallel between the systematic increase in strength and the response of the microstructure.

Although conclusive evidence supportive to an understanding of the inverse relationship between strength and toughness is limited at this point in the program, the observed trends suggest relationships which can be traced to the microstructure. A plausible explanation might be that as the strength is increased, smaller and smaller inclusions can nucleate voids. With a larger number of second-phase particles activated in the progressively higher strength levels, the resulting dimple size is seen to decrease since less void growth is necessary to link up voids. Submicron dimples on fractographs taken from the higher strength conditions indicate the possibility for void nucleation at the strengthening precipitates at some stage in the fracture process. The matrix strength and associated dislocation substructure and strengthening precipitate size and morphology are constantly changing with extent of aging. Void nucleation might then occur earlier in the stronger less tough condition wherein

localized stresses are higher for the same amount of plastic strain. The higher stresses would cause an inclusion to fail sooner. If there is a critical inclusion size criterion for failure at a given stress, a larger size distribution of inclusions will have ruptured in the stronger condition for the same amount of strain. Once formed, the growth of voids would be controlled by the flow properties of the matrix. The extent of void growth and the manner in which the voids will coalesce apparently is also controlled by stresses produced in the matrix. Submicron size strengthening precipitates may be of a critical size for failure when subject to the higher stresses present for the same amount of strain in the higher strength condition. Since the precipitates are growing in size with increasing amount of aging (strengthening), the particles tend to work towards satisfaction of the critical size criterion.

The goal is to understand the joint behavior of strength and toughness in an 18 Ni, 300 grade maraging steel. In support of this goal, the following work will be completed in the next stage of this investigation:

1. A more extensive metallographic characterization of the program alloy will be performed including optical and surface replica examination of inclusions and the martensite lath morphology. Grain size determinations will be included.

2. Inclusion identification will be performed in the scanning electron microscope with the use of the X-ray energy dispersive analyzer built into the system.

3. Quantitative microscopy will be used to assess, by type, the size and spacial distribution of the second-phase impurity inclusions present in this alloy.

4. Completion of the isothermal aging curves will provide specimens for subsequent thin foil transmission electron microscopy of the strengthening precipitates and related substructure.

5. Mechanical testing will include fatigue precracked Charpy impact tests for an assessment of toughness as a function of strength. Flow curves and general strength properties will be characterized with tension specimens.

6. Plane strain fracture toughness testing will provide toughness data and fractures which can be characterized and related to strength through fractographic techniques. Through the response of microstructure to changes in strength, a mechanism to explain the inverse relationship between strength and toughness may be proposed.

CONCLUSIONS

1. An 18 Ni, 300 grade maraging steel shows a substantial decreasing trend in fracture toughness as measured by fatigue precracked Charpy impact specimens as strength is simultaneously increased.

2. The exploratory heat of 300 grade maraging steel has failed by dimpled rupture at all strength levels observed when tested at room temperature.

3. The decrease in toughness with increase in strength can be followed fractographically with a larger size distribution of inclusions acting as void nucleation sites with increasing strength.

4. The observed dimple size is seen to decrease with increasing strength and can apparently be related to void initiation, growth and coalescence stages of plastic fracture. More work is required in order to make more definitive statements as to the mechanisms involved.

5. Fractography has suggested that strengthening precipitates, which are the result of intentional age-hardening, can act as sites for void formation. When activated, failure of the precipitates would be detrimental to toughness. More extensive thin foil, tensile sectioning and fractographic work are necessary before such speculative results can be supported.

REFERENCES

1. L. Roesch and G. Henry, Electron Microfractography, ASTM STP 453 (1969) p. 3.

2. G. J. Spaeder, R. M. Brown, and W. J. Murphy, Trans. ASM, 60 (1967) p. 418.

3. T. B. Cox and J. R. Low, Jr., "An Investigation of the Plastic Fracture of High Strength Steels," NASA Technical Report No. 5, Department of Metallurgy & Materials Science, Carnegie-Mellon University, May 1973. (See also, Met Trans., 5 (June 1974) p. 1457)

4. J. R. Low, Jr., Engr. Fract. Mech., 1 (1968) p. 47.

5. A. J. Birkle, R. P. Wei and G. E. Pellissier, Trans. ASM, 59 (1966) p. 981.

6. H. W. Antes and H. Markus, Met. Eng. Quart., 10, No. 4 (1970) p. 9.

7. Databook, Vanadium-Alloys Steel Company, "18% Nickel Ultra High Strength Maraging Steels" (1966).

8. H. J. Rack and D. Kalish, Met. Trans., 3 (1972) p. 1012.

9. T. Boniszewski and E. Boniszewski, JISI, 204 (1966) p. 360.

10. W. A. Spitzig, Journal of Materials, 5, No. 1, March 1970, p. 140.

11. T. J. Baker, Technical Note, JISI, 210 (1972) p. 793.

12. J. Gurland, Acta Met., 20 (1972) p. 735.

13. R. Henry: Private Communication, Vanadium-Alloys Steel Company, December 1973.

14. P. H. Salmon Cox, B. G. Reisdorf, and G. E. Pellissier, Trans. AIME, 239 (1967) p. 1809.

15. S. Floreen and R. F. Decker, Trans. ASM, 55 (1962) p. 518.

16. W. O. Philbrook: Private Communication, Carnegie-Mellon University, April 1974.

17. B. R. Banerjee, J. J. Hauser, and J. M. Capenos, Metal Science Journal, 2 (1968) p. 76.

18. G. R. Speich, D. S. Dabkowski, and L. F. Porter, Met. Trans., 4 (1973) p. 303.

19. W. F. Brown, Jr. and J. E. Srawley, Plane Strain Crack Toughness Testing of High Strength Metallic Materials, ASTM STP 410, ASTM (1967).

20. J. E. Srawley, M. H. Jones, and W. F. Brown, Jr., Materials Research and Standards, MTRSA, 7, No. 6 (1967) pp. 262-266.

21. S. Floreen, Metallurgical Reviews, 126 (1968) p. 115.

22. D. T. Peters, Trans. AIME, 239 (1967) p. 1981.

23. W. A. Spitzig, J. M. Chilton, and C. J. Barton, Trans. ASM, 61 (1968) p. 635.

24. J. M. Chilton and C. J. Barton, Trans. Quart. ASM, 60 (1967) p. 528.

25. T. J. Koppenaal, "Dynamic Fracture Toughness Measurements Using Pre-Cracked Charpy Samples," Aeronutronic Division of Philco-Ford Corporation, Newport Beach, Calif. (1973).

26. ASTM Standard E399-72, Annual Book of ASTM Standards, Part 31 (1972) p. 955.